

Analytical calculation of the solid angle defined by a cylindrical detector and a point cosine source with orthogonal axes

M. J. Prata¹

Instituto Tecnológico e Nuclear (ITN), Sacavém, Portugal

Abstract

We derive analytical expressions for the solid angle subtended by a right circular cylinder at a point source with cosine angular distribution in the case where the source and the cylinder axes are mutually orthogonal.

Key words: solid angle, point cosine source, cylindrical detector, cylinder

1 Introduction

The calculation of the solid angle subtended by a cylindrical detector at a point source is of common interest in nuclear science. The case of an isotropic source has been extensively studied, but, to the best of our knowledge, no work has been published considering a point cosine source. Such source could arise as the second term in a Legendre expansion of a general source or, to take a well known example, as one of the terms in the Fermi expression $\Phi(\mu) = 1 + \sqrt{3}\mu$. This expression holds for the angular distribution of low energy neutrons leaking from a variety of scattering materials and, if suitably modified ($\Phi(\mu) = 1 + A\mu$), can also be used in the case of lithium hydride (Verbinski, 1967). The scattering of neutrons from hydrogen nuclei considered at rest is also described by a cosine distribution (Ott, 1989).

In this work the situation of a point cosine source defined with respect to some axis and a right circular cylinder with axis orthogonal to that of the source

Email address: mjprata@sapo.pt (M. J. Prata).

¹ Supported by Fundação para a Ciência e Tecnologia (Programa Praxis XXI - BD/15808/98)

is considered. Under this restriction we present the analytical calculation of the solid angle subtended at the source positioned at an arbitrary location. Sample graphics of the expressions obtained are presented.

2 Solid Angle Calculation

Let the unit vector \mathbf{k} define the source direction. The source distribution $f(\boldsymbol{\Omega})$ giving the probability $f(\boldsymbol{\Omega})d\Omega$ of emission around the direction of the unit vector $\boldsymbol{\Omega}$ is defined by

$$f(\boldsymbol{\Omega}) = \begin{cases} \frac{\mathbf{k} \cdot \boldsymbol{\Omega}}{\pi} , & \mathbf{k} \cdot \boldsymbol{\Omega} \geq 0 \\ 0 , & \mathbf{k} \cdot \boldsymbol{\Omega} < 0 \end{cases} . \quad (1)$$

The distribution is normalized so that

$$\iint_{\text{all directions}} f(\boldsymbol{\Omega})d\Omega = 1 . \quad (2)$$

The solid angle (Ω) is given by

$$\Omega = \iint_{\substack{\text{directions} \\ \text{hitting detector}}} f(\boldsymbol{\Omega})d\Omega . \quad (3)$$

The origin of the coordinate system is chosen to coincide with the point source, the x axis aligned with \mathbf{k} and the z axis parallel to the cylinder axis. In figs. 1 to 3 we show the three cases to be considered and introduce some of the notation used. Generally the solid angle is a sum of two terms, the one subtended by the cylindrical surface (Ω_{cyl}) and the other by either of the end circles (Ω_{circ}). In case (i) one has $\Omega \equiv \Omega_{cyl}$, in case (ii) $\Omega \equiv \Omega_{cyl} + \Omega_{circ}$ and in case (iii), $\Omega \equiv \Omega_{circ}$. In the various cases L_1 , L_2 , d and r are all positive. From the symmetry of the problem, the solid angle is an even function of α and in the following we will thus consider $\alpha \geq 0$. In cases (i) and (ii) one has $d \geq r$ and, in case (iii), $r > d$. With the notation used there results that

$$\mathbf{k} \cdot \boldsymbol{\Omega} = \cos(\alpha + \varphi) \sin(\theta) \quad (4)$$

where θ is the polar angle from the z axis and φ is the azimuthal angle in the xy plane as measured from an axis through the origin and intersecting the

detector axis. Hence

$$\Omega = \frac{1}{\pi} \int_{\varphi_{\min}}^{\varphi_{\max}} \int_{\theta_{\min}}^{\theta_{\max}} \cos(\alpha + \varphi) \sin^2(\theta) d\theta d\varphi \quad (5)$$

where the limiting angles have yet to be determined.

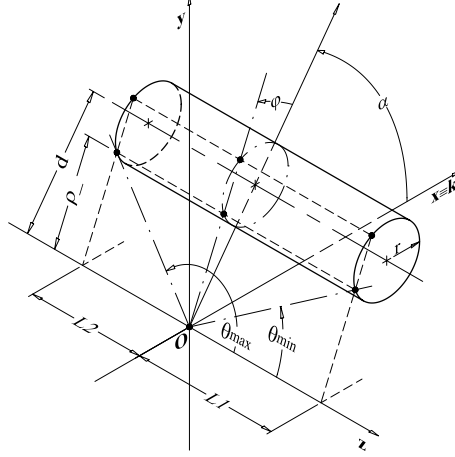


Fig. 1. Geometry in Case (i)

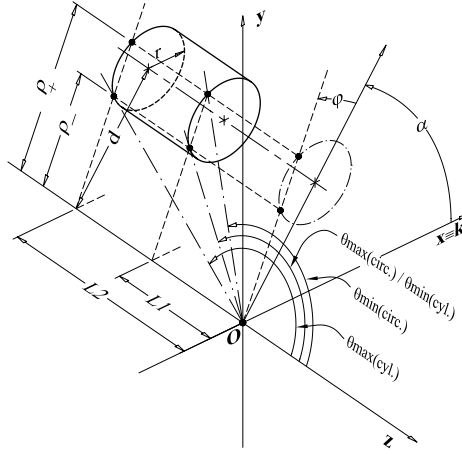


Fig. 2. Geometry in case (ii)

2.1 Integration limits

Because the source only emits into the hemisphere corresponding to $x \geq 0$, the range of variation of φ depends on the value of α , as explained in figs. 4 to 7, where the hashed area shows the *illuminated* part of the detector. Introducing

$$\varphi_0 = \arcsin(r/d) \quad , \quad (6)$$

there results

$$\alpha_1 = \pi/2 - \varphi_0 \quad (7)$$

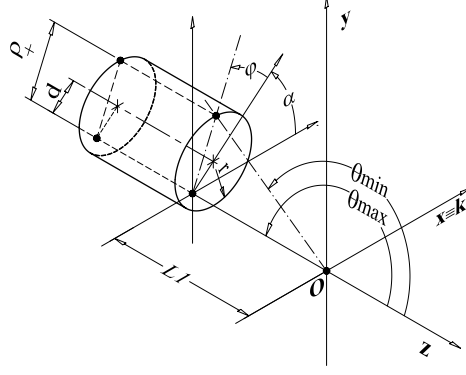


Fig. 3. Geometry in case (iii)

and

$$\alpha_c = \pi/2 + \varphi_0 . \tag{8}$$

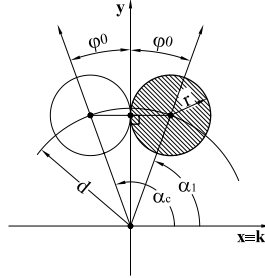


Fig. 4. Definitions of φ_0 , α_1 and α_c (cases (i) and (ii))

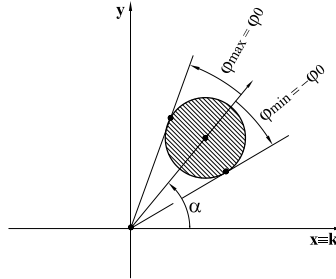


Fig. 5. Integration limits for φ in cases (i) and (ii) when $0 \leq \alpha < \alpha_1$

The limits for φ are then given in table 1.

The limits for θ can be expressed in terms of $\rho_-(\varphi)$ and $\rho_+(\varphi)$ that were introduced in the pictures and are given by

$$\rho_{\pm}(\varphi) = d \cos(\varphi) \pm \sqrt{r^2 - (d \sin(\varphi))^2} . \tag{9}$$

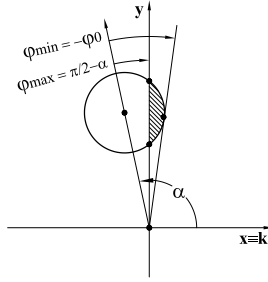


Fig. 6. Integration limits for φ in cases (i) and (ii) when $\alpha_1 \leq \alpha < \alpha_c$

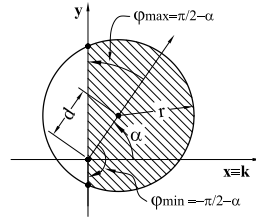


Fig. 7. Integration limits for φ in case (iii)

Table 1
Integration limits for φ

Case	α range	φ_{\min}	φ_{\max}
	$0 \leq \alpha < \alpha_1$	$-\varphi_0$	φ_0
(i) or (ii)	$\alpha_1 \leq \alpha < \alpha_c$	$-\varphi_0$	$\pi/2 - \alpha$
	$\alpha_c \leq \alpha \leq \pi$	$\Omega = 0$	
(iii)	$0 \leq \alpha \leq \pi$	$-\pi/2 - \alpha$	$\pi/2 - \alpha$

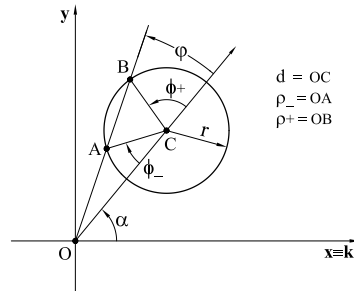


Fig. 8. Angles ϕ_{\pm} in cases (i) and (ii) ($d \geq r$)

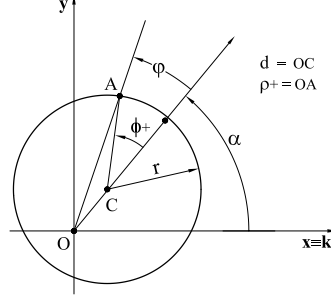


Fig. 9. Angle ϕ_+ in case (iii) ($d < r$)

Table 2
Integration limits for θ

Case	Ω_{cyl} or Ω_{circ}	θ_{\min}	θ_{\max}
(i)	Ω_{cyl}	$\pi/2 - \arctan(\frac{L_1}{\rho_-})$	$\pi/2 + \arctan(\frac{L_2}{\rho_-})$
(ii)	Ω_{cyl}	$\pi/2 + \arctan(\frac{L_1}{\rho_-})$	$\pi/2 + \arctan(\frac{L_2}{\rho_-})$
(ii)	Ω_{circ}	$\pi/2 + \arctan(\frac{L_1}{\rho_+})$	$\pi/2 + \arctan(\frac{L_1}{\rho_-})$
(iii)	Ω_{circ}	$\pi/2 + \arctan(\frac{L_1}{\rho_+})$	π

The limits for θ are summarized in table 2.

2.2 Integration

Let us define

$$f_1(L, d, r, \alpha, \varphi) \equiv f_1(\varphi) = \frac{1}{2\pi} \int \cos(\alpha + \varphi) \left[\arctan\left(\frac{L}{\rho_-}\right) + \frac{L\rho_-}{L^2 + \rho_-^2} \right] d\varphi \quad (10)$$

and

$$f_2(L, d, r, \alpha, \varphi) \equiv f_2(\varphi) = \frac{1}{2\pi} \int \cos(\alpha + \varphi) \left[\arctan\left(\frac{L}{\rho_+}\right) + \frac{L\rho_+}{L^2 + \rho_+^2} \right] d\varphi \quad (11)$$

Then, performing the first integration in the rhs of eq. 5, where θ_{\min} and θ_{\max} are given in table 2, yields in each case:

case (i)

$$\Omega = \Omega_{cyl} = [f_1(L_1, d, r, \alpha, \varphi) + f_1(L_2, d, r, \alpha, \varphi)]_{\varphi_{\min}}^{\varphi_{\max}} , \quad (12)$$

case (ii)

$$\Omega_{cyl} = [f_1(L_2, d, r, \alpha, \varphi) - f_1(L_1, d, r, \alpha, \varphi)]_{\varphi_{\min}}^{\varphi_{\max}} , \quad (13)$$

$$\Omega_{circ} = [f_1(L_1, d, r, \alpha, \varphi) - f_2(L_1, d, r, \alpha, \varphi)]_{\varphi_{\min}}^{\varphi_{\max}} , \quad (14)$$

$$\Omega = \Omega_{cyl} + \Omega_{circ} = [f_1(L_2, d, r, \alpha, \varphi) - f_2(L_1, d, r, \alpha, \varphi)]_{\varphi_{\min}}^{\varphi_{\max}} , \quad (15)$$

case (iii)

$$\Omega = \Omega_{circ} = \frac{1}{4} \int_{\varphi_{\min}}^{\varphi_{\max}} \cos(\alpha + \varphi) d\varphi - f_2(L_1, d, r, \alpha, \varphi)_{\varphi_{\min}}^{\varphi_{\max}} , \quad (16)$$

$$= \frac{1}{2} - f_2(L_1, d, r, \alpha, \varphi)_{\varphi_{\min}}^{\varphi_{\max}} . \quad (17)$$

Eq. 17 is obtained from eq. 16 by integration of the 1st term using the values from table 1.

Using again the limits from table 1, eqs. 12 to 15 and 17 can be rewritten as

case (i)

$$\Omega = \Omega_{cyl} = F_1(L_1, d, r, \alpha) + F_1(L_2, d, r, \alpha) , \quad (18)$$

case (ii)

$$\Omega_{cyl} = F_1(L_2, d, r, \alpha) - F_1(L_1, d, r, \alpha) , \quad (19)$$

$$\Omega_{circ} = F_1(L_1, d, r, \alpha) - F_2(L_1, d, r, \alpha) , \quad (20)$$

$$\Omega = \Omega_{cyl} + \Omega_{circ} = F_1(L_2, d, r, \alpha) - F_2(L_1, d, r, \alpha) , \quad (21)$$

Table 3
Definition of the integrals F_i

Integral	α range	Value	φ_{\min}	φ_{\max}
	$0 \leq \alpha < \alpha_1$	$f_i(L, d, r, \alpha, \varphi) _{\varphi_{\min}^{\max}}$	$-\varphi_0$	φ_0
F_i ($i = 1, 2$)	$\alpha_1 \leq \alpha < \alpha_c$	$f_i(L, d, r, \alpha, \varphi) _{\varphi_{\min}^{\max}}$	$-\varphi_0$	$\pi/2 - \alpha$
	$\alpha_c \leq \alpha \leq \pi$	0	-	-
F_3	$0 \leq \alpha \leq \pi$	$1/2 - f_2(L, d, r, \alpha, \varphi) _{\varphi_{\min}^{\max}}$	$-\pi/2 - \alpha$	$\pi/2 - \alpha$

case (iii)

$$\Omega = \Omega_{circ} = F_3(L_1, d, r, \alpha) , \quad (22)$$

where the integrals F_i ($i = 1..3$) are defined in table 3.

2.2.1 Calculation of F_1

Integrating by parts the 1st term in the rhs of eq. 10,

$$\begin{aligned} \int \cos(\alpha + \varphi) \arctan\left(\frac{L}{\rho_-}\right) d\varphi &= \sin(\alpha + \varphi) \arctan\left(\frac{L}{\rho_-}\right) \\ &+ \int \sin(\alpha + \varphi) \frac{L}{L^2 + \rho_-^2} \frac{d \sin(\varphi) \rho_-}{\sqrt{r^2 - [d \sin(\varphi)]^2}} d\varphi \end{aligned} \quad (23)$$

Substituting eq. 23 in the rhs of eq. 10 yields, after some algebra,

$$f_1(\varphi) = \frac{1}{2\pi} [A_{10} + \cos(\alpha)A_{11} + \sin(\alpha)A_{12}] , \quad (24)$$

where

$$A_{10} = \sin(\alpha + \varphi) \arctan\left(\frac{L}{\rho_-}\right) , \quad (25)$$

$$A_{11} = \int \frac{L\rho_-}{L^2 + \rho_-^2} \left(\cos(\varphi) + \frac{d \sin^2(\varphi)}{\sqrt{r^2 - [d \sin(\varphi)]^2}} \right) d\varphi \quad (26)$$

and

$$A_{12} = \int \frac{L\rho_-}{L^2 + \rho_-^2} \left(\frac{\rho_- \sin(\varphi)}{\sqrt{r^2 - [d \sin(\varphi)]^2}} \right) d\varphi . \quad (27)$$

Performing a change of integration variable to ϕ_- represented in fig. 8,

$$\phi_- = 2 \arctan \left(\frac{\rho_- \sin(\varphi)}{d + r - \rho_- \cos(\varphi)} \right) , \quad (28)$$

we find

$$A_{11} = Lr \int \frac{\cos(\phi_-)}{L^2 + \rho_-^2(\phi_-)} d\phi_- \quad (29)$$

and

$$A_{12} = Lr \int \frac{\sin(\phi_-)}{L^2 + \rho_-^2(\phi_-)} d\phi_- , \quad (30)$$

where

$$\rho_-(\phi_-) = \sqrt{d^2 + r^2 - 2dr \cos(\phi_-)} . \quad (31)$$

One then easily obtains

$$A_{11} = \frac{L}{2d} \left[\frac{2}{\sqrt{1-m^2}} \arctan \left(\sqrt{\frac{1+m}{1-m}} \tan \left(\frac{\phi_-}{2} \right) \right) - \phi_- \right] , \quad (32)$$

where

$$m = \frac{2dr}{L^2 + d^2 + r^2} ; 0 < m < 1 \quad (33)$$

and

$$A_{12} = \frac{L}{2d} \log(L^2 + \rho_-^2) . \quad (34)$$

2.2.2 Evaluation of F_1 ($d \neq r$)

For $0 \leq \alpha < \alpha_1$ the terms proportional to $\sin(\alpha)$ vanish and one gets

$$F_1(L, d, r, \alpha) = \frac{\cos(\alpha)}{\pi} \left[\frac{r}{d} \arctan \left(\frac{L}{\sqrt{d^2 - r^2}} \right) + \frac{L}{d} \left(\frac{1}{\sqrt{1 - m^2}} \arctan \left(\sqrt{\frac{1+m}{1-m}} \sqrt{\frac{d-r}{d+r}} \right) - \arctan \left(\sqrt{\frac{d-r}{d+r}} \right) \right) \right]. \quad (35)$$

For $\alpha_1 \leq \alpha < \alpha_c$, the expressions are less simple and we give each term in eq. 24 separately. Setting

$$\tilde{\rho}_- = \rho_-(\varphi_{\max}) = \rho_-|_{\varphi=\pi/2-\alpha} \quad (36)$$

$$= d \sin(\alpha) - \sqrt{r^2 - [d \cos(\alpha)]^2}, \quad (37)$$

the first term can be written as

$$A_{10}|_{\varphi_{\min}}^{\varphi_{\max}} = \arctan \left(\frac{L}{\tilde{\rho}_-} \right) - \arctan \left(\frac{L}{\sqrt{d^2 - r^2}} \right) \sin(\alpha - \varphi_0). \quad (38)$$

Defining

$$a_1 = \tan \left[\frac{\phi_-}{2} \right]_{\varphi_{\min}} = -\sqrt{\frac{d-r}{d+r}} \quad (39)$$

and

$$b_1 = \tan \left[\frac{\phi_-}{2} \right]_{\varphi_{\max}} = \frac{\cos(\alpha) \tilde{\rho}_-}{r + d - \sin(\alpha) \tilde{\rho}_-}, \quad (40)$$

then

$$A_{11}|_{\varphi_{\min}}^{\varphi_{\max}} = \frac{L}{2d} \left\{ \frac{2}{\sqrt{1-m^2}} \left[\arctan \left(\sqrt{\frac{1+m}{1-m}} b_1 \right) - \arctan \left(\sqrt{\frac{1+m}{1-m}} a_1 \right) \right] - 2 [\arctan(b_1) - \arctan(a_1)] \right\} \quad (41)$$

Finally, from A_{12} results

$$A_{12}|_{\varphi_{\min}}^{\varphi_{\max}} = \frac{L}{2d} \log \left[\frac{L^2 + \tilde{\rho}_-^2}{L^2 + d^2 - r^2} \right]. \quad (42)$$

Using eqs. 24, 38, 41 and 42, F_1 can be calculated in the case $\alpha_1 \leq \alpha < \alpha_c$, $d \neq r$.

2.2.3 Evaluation of F_1 ($d = r$)

The value of F_1 when $d = r$ can be obtained from eq. 10 using the integration limits from table 3 or calculating the limit of the expressions obtained in 2.2.2, for $\alpha \geq \alpha_1$. When $L \neq 0$ one obtains $F_1(L, r, r, \alpha) = (1 + \cos \alpha)/4$. Since $F_1 = 0$ for $L = 0$, F_1 is discontinuous when $r = d$, $L \rightarrow 0$.

2.2.4 Calculation of F_2

The calculation is very similar to that of F_1 . Integration by parts gives

$$\int \cos(\alpha + \varphi) \arctan\left(\frac{L}{\rho_+}\right) d\varphi = \sin(\alpha + \varphi) \arctan\left(\frac{L}{\rho_+}\right) - \int \sin(\alpha + \varphi) \frac{L}{L^2 + \rho_+^2} \frac{d \sin(\varphi) \rho_+}{\sqrt{r^2 - [d \sin(\varphi)]^2}} d\varphi . \quad (43)$$

Eq. 11 can then be rewritten as

$$f2(\varphi) = \frac{1}{2\pi} [A_{20} + \cos(\alpha)A_{21} + \sin(\alpha)A_{22}] , \quad (44)$$

where

$$A_{20} = \sin(\alpha + \varphi) \arctan\left(\frac{L}{\rho_+}\right) , \quad (45)$$

$$A_{21} = \int \frac{L\rho_+}{L^2 + \rho_+^2} \left(\cos(\varphi) - \frac{d \sin^2(\varphi)}{\sqrt{r^2 - [d \sin(\varphi)]^2}} \right) d\varphi \quad (46)$$

and

$$A_{22} = - \int \frac{L\rho_+}{L^2 + \rho_+^2} \left(\frac{\rho_+ \sin(\varphi)}{\sqrt{r^2 - [d \sin(\varphi)]^2}} \right) d\varphi . \quad (47)$$

The integration variable is now changed to ϕ_+ (fig. 8)

$$\phi_+ = 2 \arctan\left(\frac{\rho_+ \sin(\varphi)}{r - d + \rho_+ \cos(\varphi)}\right) \quad (48)$$

and the integrals are then expressed as

$$A_{21} = Lr \int \frac{\cos(\phi_+)}{L^2 + \rho_+^2(\phi_+)} d\phi_+ , \quad (49)$$

$$A_{22} = -Lr \int \frac{\sin(\phi_+)}{L^2 + \rho_+^2(\phi_+)} d\phi_+ , \quad (50)$$

where

$$\rho_+(\phi_+) = \sqrt{d^2 + r^2 + 2dr \cos(\phi_+)} . \quad (51)$$

The integration is straightforward resulting in

$$A_{21} = \frac{L}{2d} \left[\phi_+ - \frac{2}{\sqrt{1-m^2}} \arctan \left(\sqrt{\frac{1-m}{1+m}} \tan \left(\frac{\phi_+}{2} \right) \right) \right] \quad (52)$$

and

$$A_{22} = \frac{L}{2d} \log(L^2 + \rho_+^2) . \quad (53)$$

where m is obtained from eq. 33.

2.2.5 Evaluation of F_2 ($d \neq r$)

For $0 \leq \alpha < \alpha_1$ the terms proportional to $\sin(\alpha)$ again vanish giving

$$F_2(L, d, r, \alpha) = \frac{\cos(\alpha)}{\pi} \left[\frac{r}{d} \arctan \left(\frac{L}{\sqrt{d^2 - r^2}} \right) - \frac{L}{d} \left(\frac{1}{\sqrt{1-m^2}} \arctan \left(\sqrt{\frac{1-m}{1+m}} \sqrt{\frac{d+r}{d-r}} \right) - \arctan \left(\sqrt{\frac{d+r}{d-r}} \right) \right) \right] . \quad (54)$$

It is interesting that using $\arctan(z) + \arctan(1/z) = \pi/2$ the expression can be recast as

$$F_2(L, d, r, \alpha) = F_1(L, d, r, \alpha) + \cos(\alpha) L/(2d) \left(1 - 1/\sqrt{1-m^2} \right) . \quad (55)$$

For $\alpha_1 \leq \alpha < \alpha_c$, setting

$$\tilde{\rho}_+ = \rho_+(\varphi_{\max}) = \rho_+|_{\varphi=\pi/2-\alpha} \quad (56)$$

$$= d \sin(\alpha) + \sqrt{r^2 - (d \cos(\alpha))^2}, \quad (57)$$

the first term is determined from

$$A_{20}|_{\varphi_{\min}}^{\varphi_{\max}} = \arctan\left(\frac{L}{\tilde{\rho}_+}\right) - \arctan\left(\frac{L}{\sqrt{d^2 - r^2}}\right) \sin(\alpha - \varphi_0). \quad (58)$$

Considering

$$a_2 = \tan\left[\frac{\phi_+}{2}\right]_{\varphi_{\min}} = -\sqrt{\frac{d+r}{d-r}}, \quad (59)$$

$$b_2 = \tan\left[\frac{\phi_+}{2}\right]_{\varphi_{\max}} = \frac{\cos(\alpha) \tilde{\rho}_+}{r - d + \sin(\alpha) \tilde{\rho}_+}, \quad (60)$$

gives

$$A_{21}|_{\varphi_{\min}}^{\varphi_{\max}} = \frac{L}{2d} \left\{ 2 [\arctan(b_2) - \arctan(a_2)] - \frac{2}{\sqrt{1-m^2}} \left[\arctan\left(\sqrt{\frac{1-m}{1+m}} b_2\right) - \arctan\left(\sqrt{\frac{1-m}{1+m}} a_2\right) \right] \right\}. \quad (61)$$

Finally, for A_{22} the result is

$$A_{22}|_{\varphi_{\min}}^{\varphi_{\max}} = \frac{L}{2d} \log\left[\frac{L^2 + \tilde{\rho}_+^2}{L^2 + d^2 - r^2}\right], \quad (62)$$

which completes the evaluation of F_2 when $r \neq d$.

2.2.6 Evaluation of F_2 ($d = r$)

Taking the limit of the expressions obtained in 2.2.5 when $L \neq 0$, one obtains $F_2(L, r, r, \alpha = 0) = 1/2 + L/(2r)(1 - 1/\sqrt{1-m^2})$, $F_2(L, r, r, \alpha = \pi) = 0$ and

$$F_2(L, r, r, \alpha) = (1 + \cos \alpha)/4 - 1/(2\pi) \left\{ \arctan[2(r/L) \sin \alpha] + \cos(\alpha)L/r \left(\alpha - \pi + 1/\sqrt{1-m^2} \left(\pi/2 + \arctan \left[\cot(\alpha) \sqrt{1-m}/\sqrt{1+m} \right] \right) \right) - \sin(\alpha)L/(2r) \log \left[1 + 4r^2 \sin^2(\alpha)/L^2 \right] \right\}. \quad (63)$$

for $\sin(\alpha) \neq 0$. A simple calculation shows that when $L \rightarrow 0$, $F_2(L, r, r, \alpha) \rightarrow 0$, regardless of α . This is also true when $d \neq r$, and F_2 is thus continuous when $L \rightarrow 0$.

2.2.7 Calculation of F_3

From table 3,

$$F_3(L, d, r, \alpha) = 1/2 - f_2(L, d, r, \alpha, \varphi)|_{\varphi_{\min}}^{\varphi_{\max}} . \quad (64)$$

The calculation of f_2 has already been done although the quantities involved (ϕ_+ , ρ_+) have a different graphical interpretation as shown in fig. 9. Eqs. 48 and 52 can still be used but some care is required as explained further on. From eqs. 64 and 44 follows that

$$F_3 = \frac{1}{2\pi} [A_{30} + \cos(\alpha)A_{31} + \sin(\alpha)A_{32}]_{\varphi_{\min}}^{\varphi_{\max}} , \quad (65)$$

where

$$A_{30} = \varphi - A_{20} , \quad (66)$$

$$A_{31} = -A_{21} , \quad (67)$$

$$A_{32} = -A_{22} \quad (68)$$

and A_{2i} , ($i = 1..3$) are determined from eqs. 45, 52 and 53.

2.2.8 Evaluation of F_3 ($d \neq 0$)

With φ_{\max} and φ_{\min} chosen from table 1

$$\rho_+(\varphi_{\max}) = \tilde{\rho}_+ , \quad (69)$$

$$\rho_+(\varphi_{\min}) = -\tilde{\rho}_- , \quad (70)$$

where $\tilde{\rho}_-$ and $\tilde{\rho}_+$ are found from eqs. 37 and 57. To calculate $A_{31}|_{\varphi_{\min}}^{\varphi_{\max}}$ the quantities

$$a_3 = \tan \left[\frac{\phi_+}{2} \right]_{\varphi_{\min}} = \frac{\cos(\alpha) \tilde{\rho}_-}{r - d + \sin(\alpha) \tilde{\rho}_-} \quad (71)$$

and

$$b_3 = \tan \left[\frac{\phi_+}{2} \right]_{\varphi_{\max}} = \frac{\cos(\alpha) \tilde{\rho}_+}{r - d + \sin(\alpha) \tilde{\rho}_+} \quad (72)$$

will be useful. A_{30} is given by

$$A_{30}|_{\varphi_{\min}}^{\varphi_{\max}} = \pi - [\arctan(L/\tilde{\rho}_+) - \arctan(L/\tilde{\rho}_-)] . \quad (73)$$

Using eq. A.1 from the appendix results in

$$A_{30}|_{\varphi_{\min}}^{\varphi_{\max}} = \pi - 2 \arctan(1/z) , \quad (74)$$

where

$$z = \frac{r^2 - d^2 - L^2 + \sqrt{(r^2 - d^2 - L^2)^2 + 4L^2(r^2 - [d \cos(\alpha)]^2)}}{2L\sqrt{r^2 - [d \cos(\alpha)]^2}} . \quad (75)$$

Then, applying $\arctan(z) + \arctan(1/z) = \pi/2$ yields

$$A_{30}|_{\varphi_{\min}}^{\varphi_{\max}} = 2 \arctan(z) . \quad (76)$$

Some care is required to obtain A_{31} . From fig. 9 is clear that as $\alpha \rightarrow \pi/2$ then $\phi_+(\varphi_{\min}) \rightarrow -\pi$ and that $-\pi < \phi_+(\varphi_{\min}) < -3\pi/2$ for $\alpha > \pi/2$. Therefore $a_3 = \tan[\phi_+(\varphi_{\min})/2]$ is not continuous as α goes through $\pi/2$. The discontinuity also appears in the rhs of eq. 48 when φ decreases to less than $-\pi$. From eqs. 67 and 52 its obvious that both terms in A_{31} will be discontinuous. The integral, of course, must be continuous and a proper expression can be provided by noticing that while

$$z \neq \arctan[\tan(z)] ; -\pi < z < -\pi/2 , \quad (77)$$

one has

$$z = -\pi/2 - \arctan[1/\tan(z)] ; -\pi < z < 0 . \quad (78)$$

Thus, to evaluate A_{31} , the substitutions

$$\arctan(a_3) \rightarrow -\pi/2 - \arctan(1/a_3) , \quad (79)$$

$$\arctan\left(\sqrt{\frac{1-m}{1+m}}a_3\right) \rightarrow -\pi/2 - \arctan\left[1/\left(\sqrt{\frac{1-m}{1+m}}a_3\right)\right] , \quad (80)$$

are used and it is found that

$$A_{31}|_{\varphi_{\min}}^{\varphi_{\max}} = -\frac{L}{2d} \left\{ 2 [\pi/2 + \Delta t_1] - \frac{2}{\sqrt{1-m^2}} [\pi/2 + \Delta t_2] \right\}, \quad (81)$$

where

$$\Delta t_1 = \arctan(b_3) + \arctan(1/a_3), \quad (82)$$

$$\Delta t_2 = \arctan\left(\sqrt{\frac{1-m}{1+m}}b_3\right) + \arctan\left(\sqrt{\frac{1+m}{1-m}}/a_3\right). \quad (83)$$

The sum of arctangents can be cast as a single one using eq. A.1 from the appendix and after some algebra one gets

$$\Delta t_1 = 2 \arctan [d \cos(\alpha) / (r + E)], \quad (84)$$

$$\Delta t_2 = 2 \arctan \left[\{Gd \cos(\alpha)\} / \left\{EH + r\sqrt{H^2 - [2Ld \cos(\alpha)]^2}\right\} \right], \quad (85)$$

where

$$E = \sqrt{r^2 - [d \cos(\alpha)]^2}, \quad (86)$$

$$G = L^2 + d^2 - r^2 \quad (87)$$

and

$$H = \sqrt{[L^2 + (d+r)^2] [L^2 + (d-r)^2]}. \quad (88)$$

The remaining term is given by

$$A_{32}|_{\varphi_{\min}}^{\varphi_{\max}} = -\frac{L}{2d} \log \left(\frac{L^2 + \tilde{\rho}_+^2}{L^2 + \tilde{\rho}_-^2} \right). \quad (89)$$

2.2.9 Evaluation of F_3 ($d = 0$)

Calculation of the limit of the expressions obtained in 2.2.8 yields $F_3(L, d = 0, r, \alpha) = 1/2 - (\arctan [L/r] + Lr / (L^2 + r^2))$. In the same way one can show

that $F_3(L \rightarrow 0, d < r, r, \alpha) = 1/2$ regardless of d , r and α . Although F_3 is only needed for $d < r$, it is worth mentioning that $\lim_{L \rightarrow 0} (\lim_{d \rightarrow r^-} F_3(L, d, r, \alpha)) = 1/4(1 + \cos \alpha)$.

3 Sample graphics and discussion

To illustrate the behavior with respect to α we consider a cylinder of length 10 and radius 1. In figs. 10, 11 and 12 are shown examples of cases (i),(ii) and (iii), respectively. As argued before, Ω is an even function of α in all cases. In cases (i) and (ii), for $0 \leq |\alpha| < \pi/2 - \arcsin(r/d)$, the solid angle is *simply proportional to $\cos(\alpha)$* ; for $|\alpha| > \pi/2 + \arcsin(r/d)$, $\Omega = 0$. In between, the dependence on α is more complicated because a fraction of the cylinder is not illuminated by the source, but $\Omega(\alpha)$ obviously decreases as $|\alpha|$ increases. The transition region is large for $d \approx r$ ($d < r$) and becomes increasingly narrower as d increases. For $d \gg r$, the region essentially vanishes so that $\Omega \propto \cos(\alpha)$ when $|\alpha| \lesssim \pi/2$ and $\Omega = 0$ when $|\alpha| \gtrsim \pi/2$. It is intuitive that in case (i), Ω decreases when distance d increases and all other parameters are held constant. This is not necessarily true for case (ii), because source and cylinder are in a skew geometry. Considering two distances $d_1 < d_2$, one concludes from the preceding discussion that there is certainly some region for α where $\Omega(d_2) = 0$ and $\Omega(d_1) > 0$ so that $\Omega(d_1) > \Omega(d_2)$. As $|\alpha|$ decreases to 0, this relation *can* be inverted, which happens for all distances shown in fig. 11. Since for very large d , Ω is certainly a decreasing function of d , there must be a maximum, for each α . This is illustrated in fig. 13, for $\alpha = 0$, $L_1 = 5$ and two cylinder lengths: 10 ($L_2 = 15$) and 20 ($L_2 = 25$). It is worth mentioning that in case (ii), apart from the α dependence, a similar behavior can be observed for an isotropic point source (i.e. a maximum when d is changed and L_1 and L_2 kept constant). Case (iii) is exemplified in fig. 12. In this case ($r > d$) the solid angle is defined only by one the end circles which is, in general, partially illuminated by the source. The exception happens when $d \rightarrow r$: for $\alpha = 0$ the circle is fully illuminated where as for $\alpha = \pi$ it is totally obscured. When $d = 0$ the source is aligned with the center of circle and Ω is then independent of α . As d increases, for $L_1 \neq 0$, the dependence on α becomes stronger with a maximum when $\alpha = 0$. When $L_1 = 0$ (not shown in fig. 12), $\Omega = 1/2$, regardless of α or d .

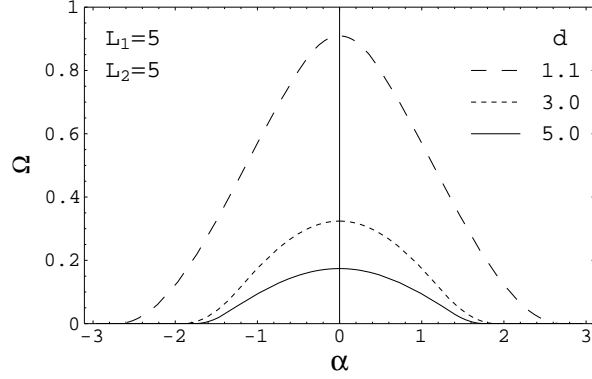


Fig. 10. Solid angle in case (i), for a cylinder with radius 1 and length $10 = 5 + 5$

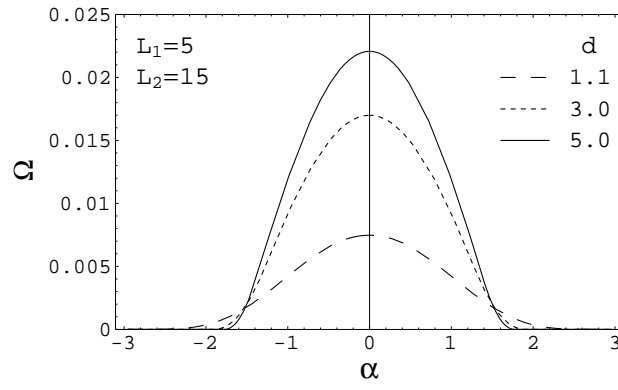


Fig. 11. Solid angle in case (ii) for a cylinder with radius 1 and length $10 = 15 - 5$

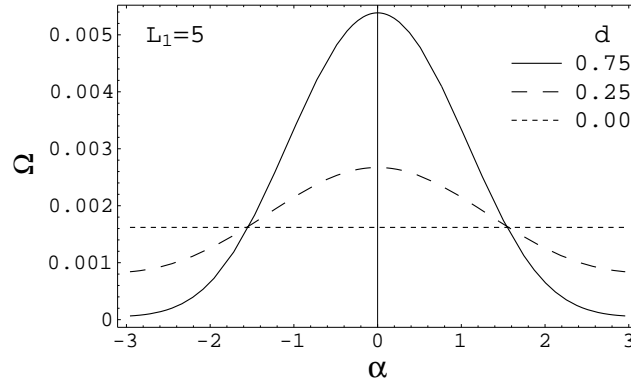


Fig. 12. Solid angle in case (iii) when $\Omega = \Omega_{circ}$, for a circle with radius 1. The intersection of the three curves near $\pi/2$ is not exact.

4 Conclusions and outlook

The solid angle defined by a point cosine source and a right circular cylinder with axis orthogonal to that of the source has been treated analytically. It has been shown that for $d > r$ and $0 \leq |\alpha| < \pi/2 - \arcsin(r/d)$, the whole dependence on α is given by a $\cos(\alpha)$ factor (eqs. 35 and 54). It is possible

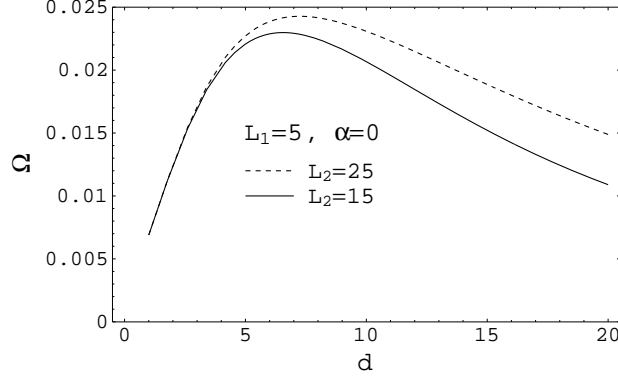


Fig. 13. Peak values ($\alpha = 0$) of the solid angle in case (ii) as a function of d , for two cylinders of radius 1 and lengths 10 ($15 - 5$) and 20 ($25 - 5$)

to obtain, in a similar fashion, analytical expressions in the case of a cosine source distributed on a wire parallel to the cylinder axis. A work where we report these results is in preparation.

Acknowledgements

I would like to thank João Prata for his thorough review of the manuscript.

A Sum of Arctans

To prove the identity

$$\arctan x \pm \arctan y = 2 \arctan \left[\frac{(x \pm y)}{\left(1 \mp xy + \sqrt{(x \pm y)^2 + (1 \mp xy)^2}\right)} \right] \quad (\text{A.1})$$

consider $h(x, y) = \arctan x \pm \arctan y$ and $g(x, y) = 2 \arctan [(x \pm y) / D]$ where

$$D = \left(1 \mp xy + \sqrt{(x \pm y)^2 + (1 \mp xy)^2}\right) .$$

Using $\tan(u \pm v) = [\tan(u) \pm \tan(v)] / [1 \mp \tan(u) \tan(v)]$, we find that $\tan(h) = (x \pm y) / (1 \mp xy)$. In a similar way, applying $\tan(2u) = 2 \tan(u) / [1 - \tan^2(u)]$, gives

$$\begin{aligned} \tan [g(x, y)] &= 2 \frac{(x \pm y) / D}{\left[D^2 - (x \pm y)^2\right] / D^2} \\ &= (x \pm y) / (1 \mp xy) , \end{aligned}$$

where in the last step we used the fact that $D \neq 0$. Since $\tan(h) = \tan(g)$ then $h - g = n\pi$ for some n . Taking $x = y = 0$ results that $n = 0$ and, because h and g are continuous, we conclude that eq. A.1 holds for any x and y .

References

- Ott, K.O., Bezella, W.A., 1989. Introductory Nuclear Reactor Statics. American Nuclear Society, La Grange Park, (p.170).
- Verbinski, V.V., 1967. Angular Distributions of Low-Energy Neutrons Leaking from Various Scattering Materials. Nucl. Sci. Eng. 27, 67-69.